

# Supporting Information for ”Exploiting SMILEs and CMIP5 Archive to understand Arctic Climate Change Seasonality and Uncertainty”

You-Ting Wu<sup>1</sup>, Yu-Chiao Liang<sup>1,2</sup>, Yan-Ning Kuo<sup>3</sup>, Flavio Lehner<sup>3,4</sup>, Michael Previdi<sup>2</sup>, Lorenzo M. Polvani<sup>2,5,6</sup>, Min-Hui Lo<sup>1</sup>, and Chia-Wei Lan<sup>1</sup>

<sup>1</sup>Department of Atmospheric Sciences, National Taiwan University, Taipei, Taiwan

<sup>2</sup>Lamont-Doherty Earth Observatory, Columbia University, Palisades, NY, USA

<sup>3</sup>Department of Earth and Atmospheric Sciences, Cornell University, Ithaca, USA

<sup>4</sup>Climate and Global Dynamics Laboratory, National Center for Atmospheric Research, Boulder, CO, USA

<sup>5</sup>Department of Earth and Environmental Sciences, Columbia University, New York, NY, USA

<sup>6</sup>Department of Applied Physics and Applied Mathematics, Columbia University, New York, NY, USA

## Contents of this file

1. Moisture Budget Analysis
2. Energy Budget Analysis

3. Table S1

4. Figures S1 to S6

## 1. Moisture budget analysis

Previous studies have used this method to investigate the drivers of regional or global precipitation change under global warming (e.g., Chou & Lan, 2012; Lan et al., 2016; Liang et al., 2020). The moisture budget is formulated as

$$\Delta P = \Delta(-\langle \vec{V}_h \cdot \nabla q \rangle) + \Delta(-\langle \omega \partial_p q \rangle) + \Delta SLHF + \Delta \delta, \quad (1)$$

where  $P$  denotes the total precipitation,  $\vec{V}_h$  the horizontal wind field,  $q$  the specific humidity,  $\omega$  the vertical velocity in pressure coordinates,  $SLHF$  the surface latent heat flux, and  $\delta$  the residuals.  $\langle \rangle$  indicates the mass integration from the surface to top of the model. The first term on the right hand side ( $-\langle \vec{V}_h \cdot \nabla q \rangle$ ) is the horizontal moisture advection, while the second term ( $-\langle \omega \partial_p q \rangle$ ) is the vertical moisture advection.  $\Delta$  represents the difference between each 30-year period and the reference period (1951-1980) for each month, and the units here are  $\text{Wm}^{-2}$ .

## 2. Energy budget analysis

To investigate the underlying mechanisms driving Arctic near-surface temperature change, we analyze the top of atmosphere (TOA) energy budget. The budget is formulated as:

$$\Delta R + \Delta F - \Delta H = 0, \quad (2)$$

where  $R$  is the net TOA radiation,  $F$  is the horizontal convergence of heat transport, and  $H$  is the net heat uptake. The units of each term are  $\text{Wm}^{-2}$ .

The change of heat transport,  $\Delta F$ , is decomposed into atmospheric and oceanic components:

$$\Delta F = \Delta AHT + \Delta OHT, \quad (3)$$

where  $\Delta AHT$  and  $\Delta OHT$  are the changes of atmospheric and oceanic heat flux convergence, respectively. The change of heat uptake,  $\Delta H$ , is estimated as the change of oceanic heat uptake assuming negligible heat capacity of the atmosphere and land.  $\Delta H$ , thus, is decomposed into:

$$\Delta H = \Delta OHT - \Delta OHR, \quad (4)$$

where  $\Delta OHR$  is the change of oceanic heat release (positive into the atmosphere), and  $\Delta OHT$  is calculated as the residual term in Equation 4.  $\Delta OHR$  is further decomposed into:

$$\Delta OHR = \Delta THF + \Delta LW + \Delta SW, \quad (5)$$

where  $\Delta THF$  is the change of turbulent heat flux (latent heat plus sensible heat), and  $\Delta LW$  and  $\Delta SW$  represent the changes of net longwave and shortwave radiation at the surface, respectively.

For the change of net radiation at TOA ( $\Delta R$ ), we use the radiative kernels (Soden et al., 2008; Pendergrass et al., 2018) to decompose it into the change of radiative forcing of CO<sub>2</sub> ( $\Delta Q$ ) and the sum of climate feedbacks ( $\Sigma \lambda_i \Delta T_s$ ):

$$\Delta R = \Delta Q + \Sigma \lambda_i \Delta T_s, \quad (6)$$

where  $\Delta T_s$  is the change of Arctic near-surface air temperature, and  $\lambda_i$  represents for the radiative feedback parameter of different components, including the surface albedo ( $ALB$ ), the Planck ( $PL$ ), the lapse-rate ( $LR$ ), the water vapor ( $WV$ ), the shortwave cloud ( $SWC$ ), and the longwave cloud ( $LWC$ ) feedbacks, respectively. Due to lack of data, the moisture and energy budget analyses are only performed with CESM1-CAM5 SMILE.



**Table S1.** List of CMIP5 global climate models and ensemble members used in this study.

	Name	Member
1.	CanESM2	r1i1p1
2.	CCSM4	r1i1p1
3.	CESM1-CAM5	r1i1p1
4.	CNRM-CM5	r1i1p1
5.	CSIRO-Mk3.6.0	r1i1p1
6.	FGOALS-g2	r1i1p1
7.	GISS-E2-H	r1i1p1
8.	GISS-E2-R	r1i1p1
9.	HadGEM2-AO	r1i1p1
10.	HadGEM2-ES	r1i1p1
11.	MIROC-ESM	r1i1p1
12.	MIROC-ESM-CHEM	r1i1p1
13.	MIROC5	r1i1p1
14.	MPI-ESM-LR	r1i1p1
15.	MPI-ESM-MR	r1i1p1
16.	MRI-CGCM3	r1i1p1
17.	NorESM1-ME	r1i1p1
18.	NorESM1-M	r1i1p1

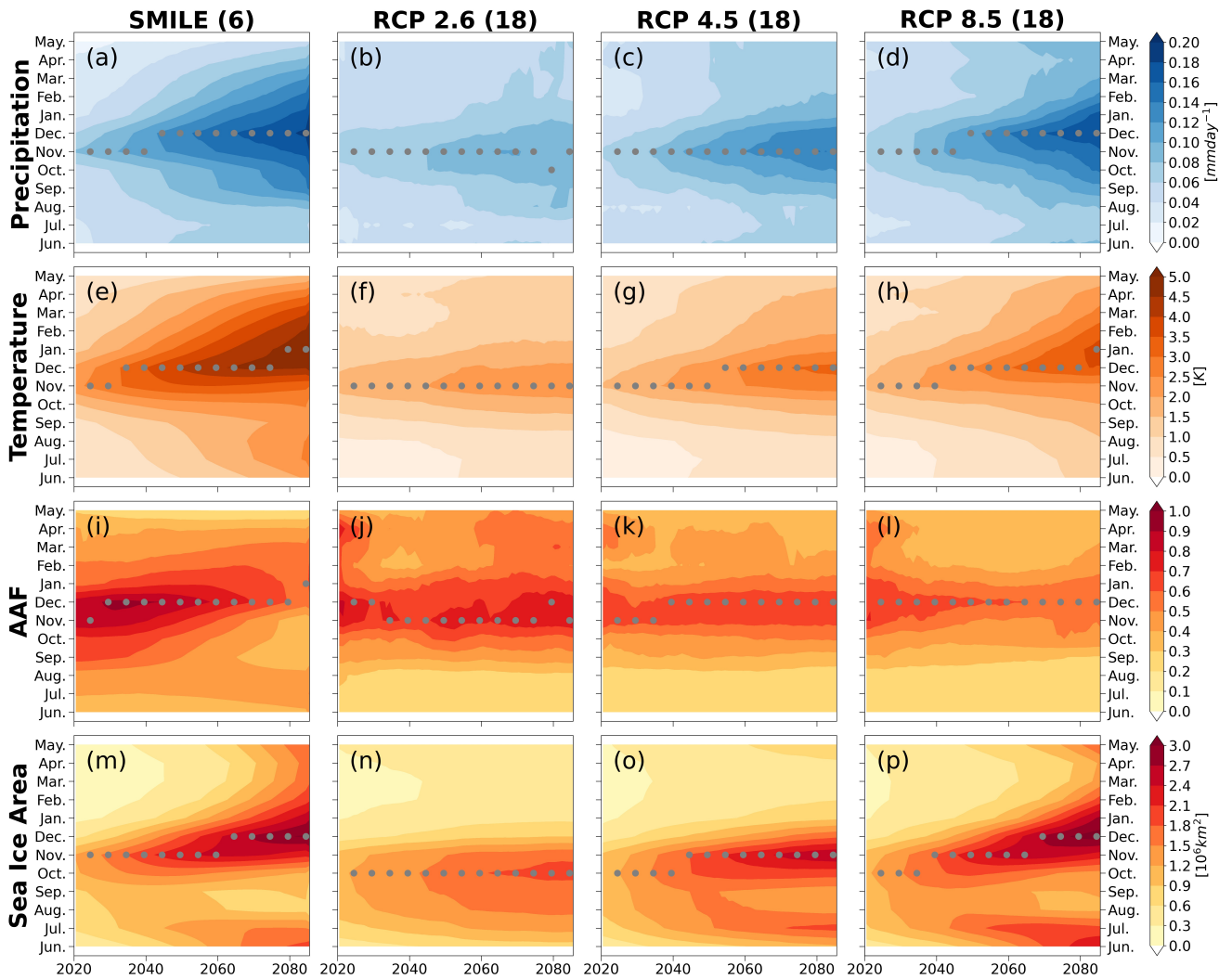


**Figure S1.** Standard deviation across models in the projection of Arctic precipitation response using (a) SMILEs, (b) CMIP5 models under RCP2.6 scenario, (c) CMIP5 models under RCP4.5 scenario, and (d) CMIP5 models under RCP8.5 scenario. (e)-(h) As in (a)-(d), but for Arctic surface air temperature response. (i)-(l) As in (a)-(d), but for the AAF. (m)-(p) As in (a)-(d), but for Arctic SIA response. Years along the x-axis denote the centers of each 30-year period. Grey dots denote the annual maximum values every 5 years. Values in parentheses in the titles of (a)-(d) indicate the number of models for each dataset.

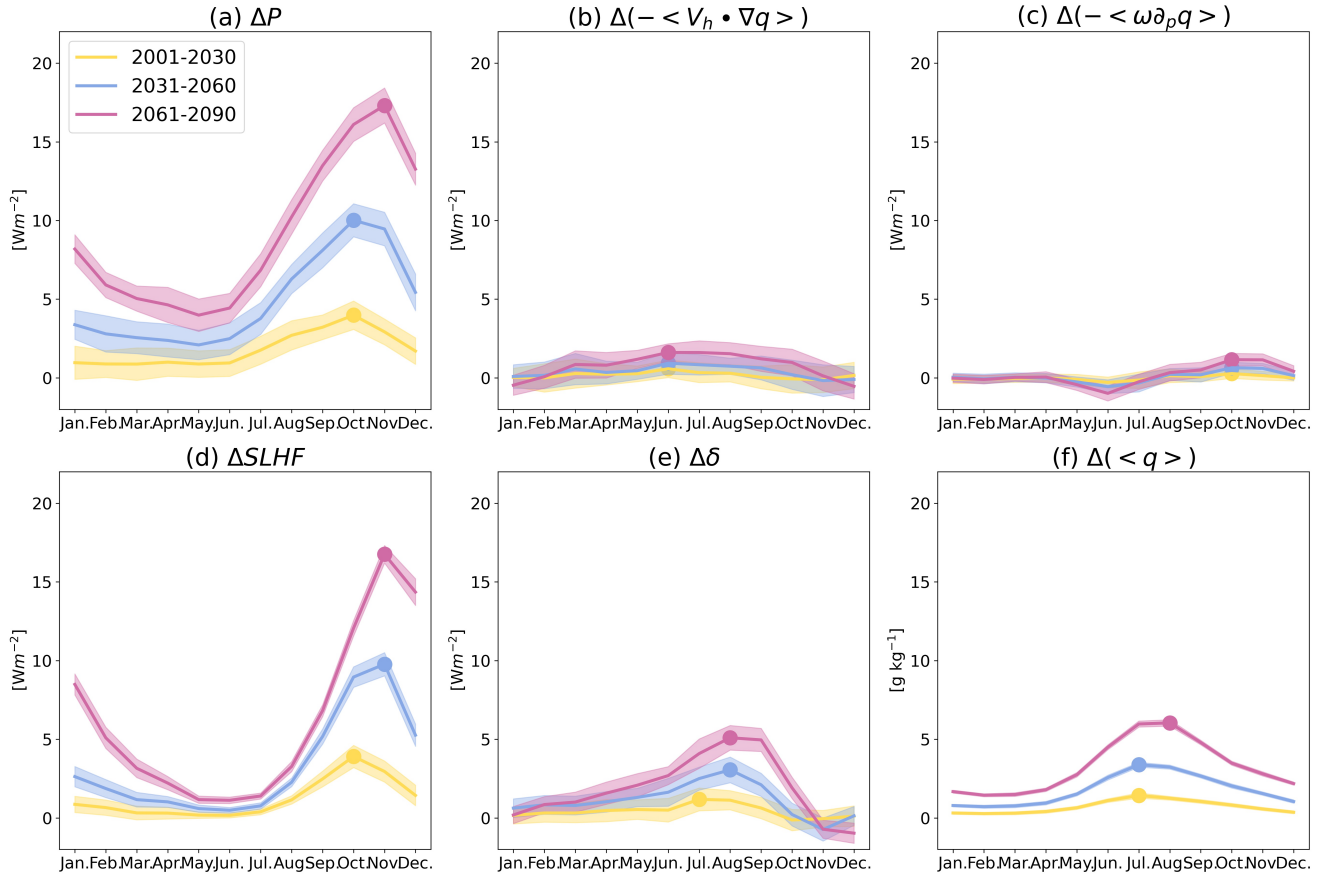


**Figure S2.** The seasonal evolution the changes in precipitation (in  $\text{Wm}^{-2}$ ), and it components from the moisture budget, over the Arctic domain for CESM1-CAM5. (a) The precipitation change  $\Delta P$ , (b) the horizontal moisture advection, (c) the vertical moisture advection, (d) the surface latent heat flux, (e) the residual, and (f) the integrated specific humidity from bottom to top of the atmosphere. All values are referenced to the 1951-1980 mean value. The solid lines indicate ensemble mean, while color shading represents the range of one standard deviation across the ensemble. Dots denote the maximum values within each period.

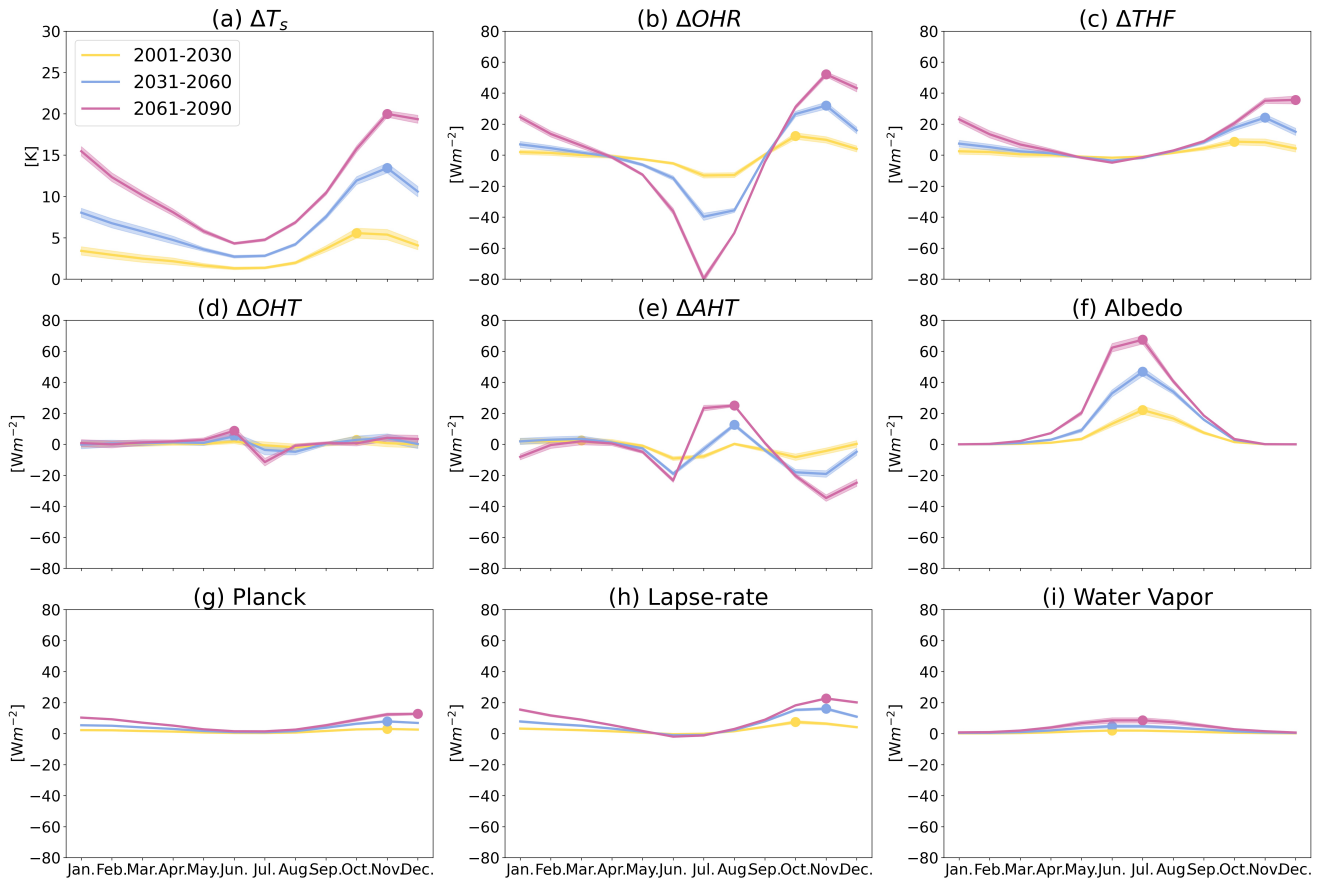


**Figure S3.** The seasonal evolution of the changes in surface temperature (in K), and its decomposition over the Arctic domain for CESM1-CAM5. (a) Arctic near-surface temperature change, (b) oceanic heat release, (c) turbulent heat flux, (d) oceanic heat transport, (e) atmospheric heat transport, (f) surface albedo feedback, (g) Planck feedback, (h) lapse-rate feedback, and (i) water vapor feedback. All values are reference to the 1951-1980 mean value. The solid lines indicate the ensemble mean, while the color shading represents the range of one standard deviation across the ensemble. Dots denote the maximum values within each period.

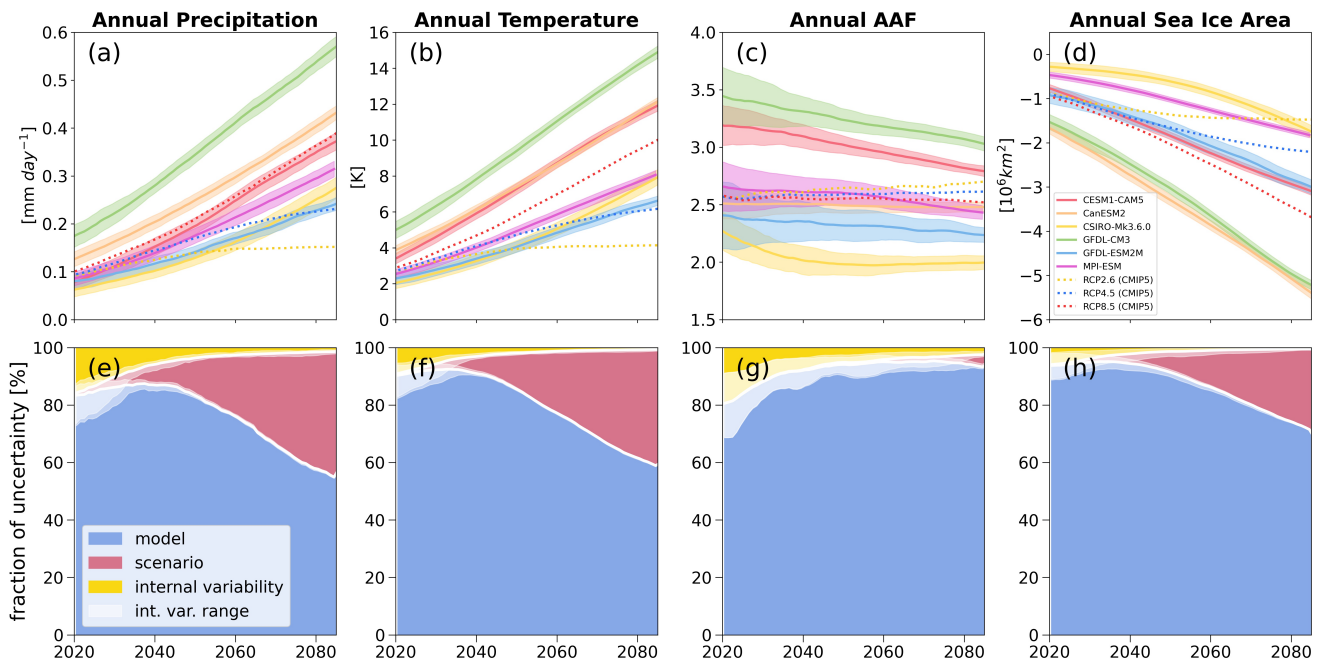


**Figure S4.** (a)-(d) Time series of annual (a) Arctic precipitation, (b) Arctic SAT, (c) AAF, and (d) Arctic SIA, computed using 6 SMILEs and 3 CMIP5 scenarios. Values are changes relative to mean of 1951-1980. The solid lines indicate the ensemble means, while the color shading represents the range of one standard deviation across each ensemble, and the dashed lines represent the multi-model mean for each scenario in CMIP5. (e)-(h) The fraction of uncertainty for annual (e) Arctic precipitation, (f) Arctic SAT, (g) AAF, and (h) Arctic SIA. In each panel, the blue shading represents the model structural uncertainty, the red shading the emissions scenario uncertainty, and the yellow shading the internal variability uncertainty. The white solid lines represent the margins of each decomposed uncertainty, and white shading indicates the range of internal variability determined by the maximum and minimum values.

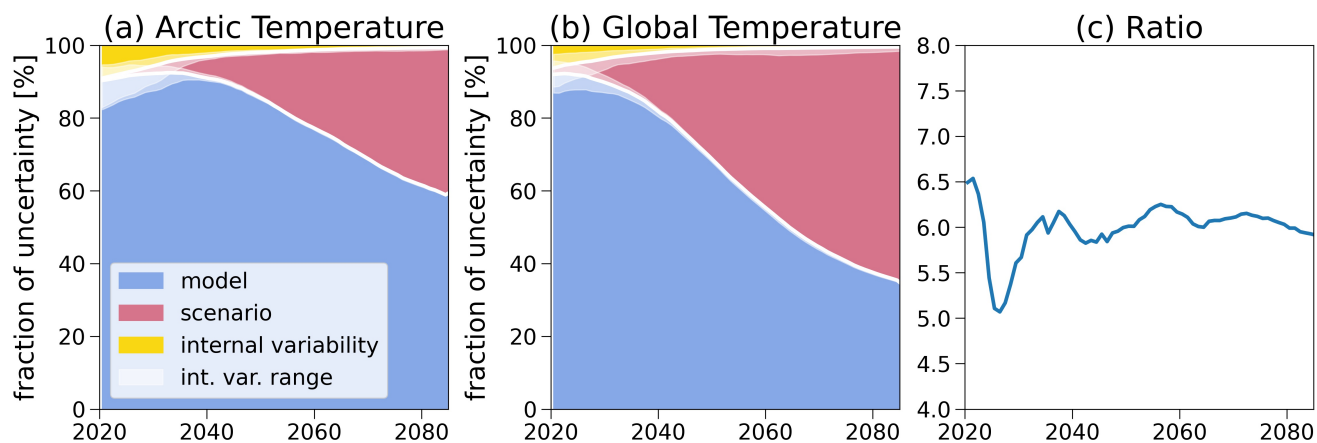


**Figure S5.** (a) The fraction of uncertainty for annual Arctic surface air temperature (SAT) response. (b) As in (a), but for global SAT response. In each panel, the blue shading represents the model structural uncertainty, the red shading the emissions scenario uncertainty, and the yellow shading the internal variability uncertainty. The white solid lines represent the margins of each decomposed uncertainty, and white shading indicates the range of internal variability determined by the maximum and minimum values. (c) Time series of ratio between the scenario uncertainty in Arctic SAT responses and that in global SAT responses.

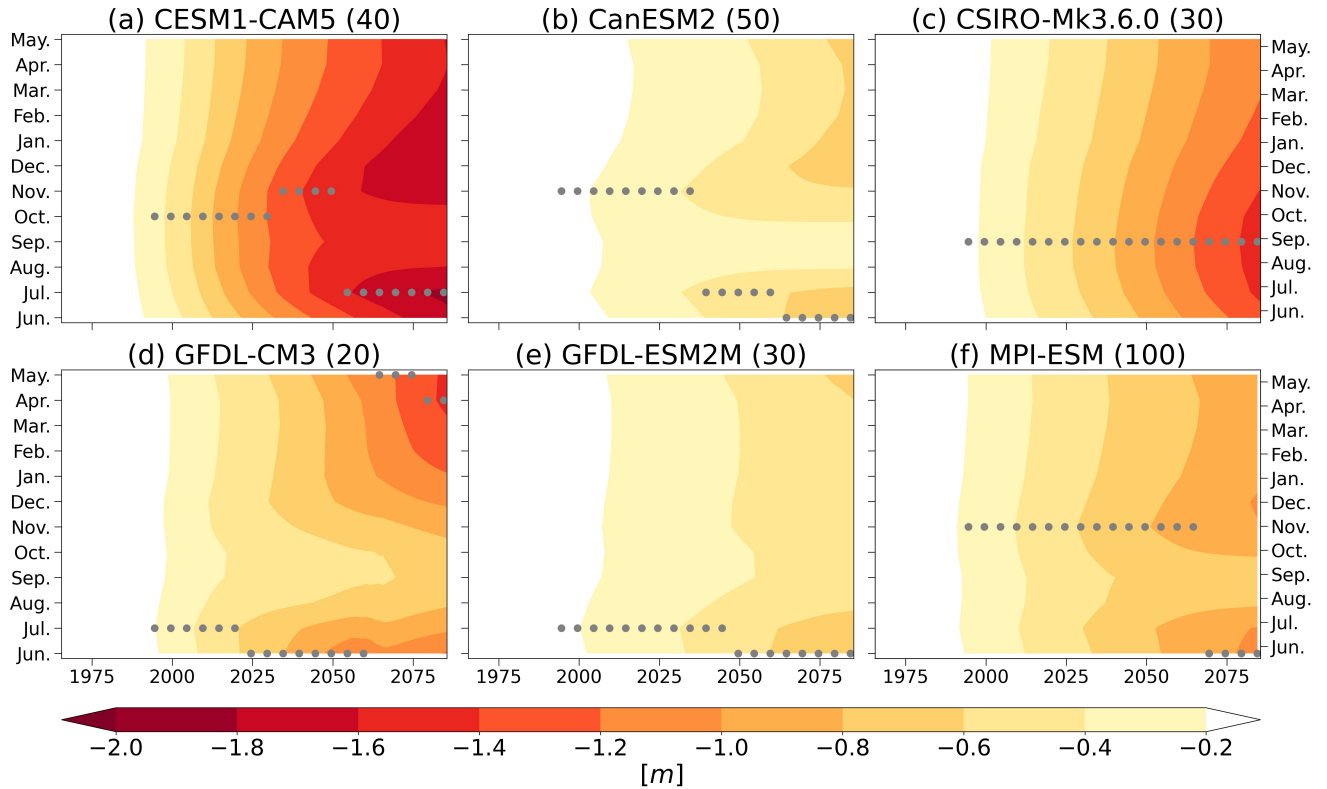


**Figure S6.** Seasonal evolutions of (a)-(f) sea-ice thickness responses averaged over the Arctic domain ( $70^{\circ}\text{N}$ - $90^{\circ}\text{N}$ ) for six SMILEs. Values in each panel are the ensemble mean during 30-year periods relative to the 1951-1980 ensemble mean. Years along the x-axis denote the centers of each 30-year period, and dots denote the annual maximum values every 5 years. The number of ensemble members in each SMILE is indicated in parentheses.

## References

- Chou, C., & Lan, C.-W. (2012). Changes in the annual range of precipitation under global warming. *Journal of Climate*, *25*(1), 222–235.
- Lan, C.-W., Lo, M.-H., Chou, C., & Kumar, S. (2016). Terrestrial water flux responses to global warming in tropical rainforest areas. *Earth's Future*, *4*(5), 210–224.
- Liang, Y.-C., Lo, M.-H., Lan, C.-W., Seo, H., Ummenhofer, C. C., Yeager, S., . . . Steffen, J. D. (2020). Amplified seasonal cycle in hydroclimate over the amazon river basin and its plume region. *Nature communications*, *11*(1), 1–11.
- Pendergrass, A. G., Conley, A., & Vitt, F. M. (2018). Surface and top-of-atmosphere radiative feedback kernels for cesm-cam5. *Earth System Science Data*, *10*(1), 317–324.
- Soden, B. J., Held, I. M., Colman, R., Shell, K. M., Kiehl, J. T., & Shields, C. A. (2008). Quantifying climate feedbacks using radiative kernels. *Journal of Climate*, *21*(14), 3504–3520.